SIX2 Regulates Human β Cell Differentiation from Stem Cells and Functional Maturation *In Vitro*
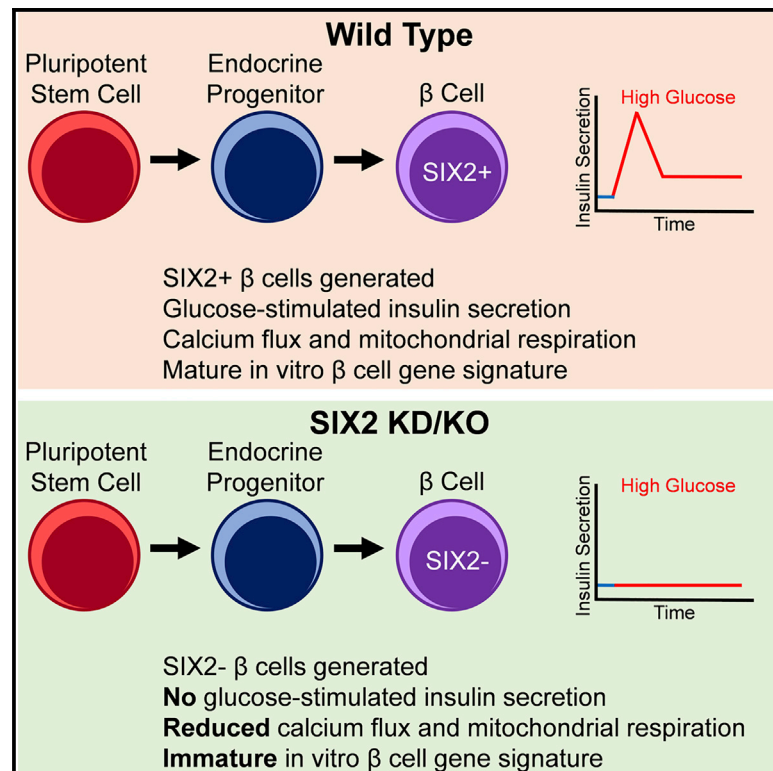
Graphical Abstract

Highlights

- SIX2 regulates the functional maturation of stem cell-derived β cells

- Knockdown and knockout of SIX2 impairs static and dynamic GSIS

- SIX2 regulates *in vitro* β cell gene expression signature

- SIX2 expression is heterogeneous within the SC-β cell population

Authors

Leonardo Velazco-Cruz,
Madeleine M. Goedegebuure,
Kristina G. Maxwell,
Punn Augsornworawat,
Nathaniel J. Hogrebe, Jeffrey R. Millman

Correspondence

jmillman@wustl.edu

In Brief

Velazco-Cruz et al. characterize the role of SIX2 in stem cell differentiation to β cells. SIX2 expression is restricted to late-stage endocrine cells. Generation of β cells does not require SIX2, but lack of SIX2 impairs maturation, as assessed by glucose-stimulated insulin secretion, calcium flux, mitochondrial respiration, and gene expression.

Report

SIX2 Regulates Human β Cell Differentiation from Stem Cells and Functional Maturation *In Vitro*

Leonardo Velazco-Cruz,[1] Madeleine M. Goedegebuure,[1] Kristina G. Maxwell,[1,2] Punn Augsornworawat,[1,2] Nathaniel J. Hogrebe,[1] and Jeffrey R. Millman[1,2,3,*]

[1]Division of Endocrinology, Metabolism, and Lipid Research, Washington University School of Medicine, St. Louis, MO 63110, USA
[2]Department of Biomedical Engineering, Washington University in St. Louis, St. Louis, MO 63130, USA
[3]Lead Contact
*Correspondence: jmillman@wustl.edu
 https://doi.org/10.1016/j.celrep.2020.107687

SUMMARY

Generation of insulin-secreting β cells *in vitro* is a promising approach for diabetes cell therapy. Human embryonic stem cells (hESCs) and human induced pluripotent stem cells (hiPSCs) are differentiated to β cells (SC-β cells) and mature to undergo glucose-stimulated insulin secretion, but molecular regulation of this defining β cell phenotype is unknown. Here, we show that maturation of SC-β cells is regulated by the transcription factor SIX2. Knockdown (KD) or knockout (KO) of *SIX2* in SC-β cells drastically limits glucose-stimulated insulin secretion in both static and dynamic assays, along with the upstream processes of cytoplasmic calcium flux and mitochondrial respiration. Furthermore, SIX2 regulates the expression of genes associated with these key β cell processes, and its expression is restricted to endocrine cells. Our results demonstrate that expression of SIX2 influences the generation of human SC-β cells *in vitro*.

INTRODUCTION

Pancreatic β cells regulate blood glucose levels by secreting a precise amount of insulin in response to changes in extracellular glucose, and death or dysfunction of these cells results in diabetes. Transplantation of insulin-secreting cells shows promise to be an effective treatment for diabetes (Bellin et al., 2012; McCall and Shapiro, 2012; Millman and Pagliuca, 2017), and a small number of patients who have received such implants from cadaveric donors remain normoglycemic for years. Scarcity and high variability of donor islets limit this approach, however (McCall and Shapiro, 2012).

To overcome this limitation, strategies for specifying β cells from human embryonic stem cells (hESCs) *in vitro* have been described recently (Pagliuca et al., 2014; Rezania et al., 2014). These approaches use growth factors and small molecules to mimic native β cell development by first specifying definitive endoderm (D'Amour et al., 2005), followed by the generation of NKX6-1[+] pancreatic progenitors (D'Amour et al., 2006). These progenitors are specified into endocrine via the expression of NEUROG3 (NGN3) (Gu et al., 2002) and are subsequently matured into SC-β cells and other islet endocrine cell types (Veres et al., 2019). More recent studies have defined conditions that greatly improve the functional maturation of SC-β cells, achieving first- and second-phase insulin secretion (Hogrebe et al., 2020; Velazco-Cruz et al., 2019). While a large number of genes that temporally correlate with maturation have been identified (Nair et al., 2019; Veres et al., 2019), the molecular mechanisms controlling this functional maturation are unclear, hampering further improvements in function.

To investigate the functional maturation of human β cells *in vitro*, we studied the homeobox transcription factor SIX2 during differentiation to SC-β cells. SIX2 is not expressed in rodent β cells (Segerstolpe et al., 2016; Xin et al., 2016), which limits the use of conventional approaches for its study, including commonly used insulinoma cell lines and animal models. SIX2 has recently been identified as being expressed in human β cells and linked to type 2 diabetes and aging (Arda et al., 2016; Hachiya et al., 2017; Kim et al., 2011; Spracklen et al., 2018).

Here, we report that SIX2 is key for generating functional SC-β cells *in vitro*. Using short hairpin RNA (shRNA) and CRISPR-Cas9 to knock down (KD) SIX2 expression or knock out (KO) the *SIX2* gene, respectively, we show that both static and dynamic glucose-stimulated insulin secretion are severely hampered with reduced SIX2 expression. Upstream processes of cytoplasmic calcium flux and mitochondrial respiration are similarly reduced. Using RNA sequencing, we observe a large number of genes associated with maturation and β cell function to be reduced with the KD of SIX2, including gene sets associated temporally with SC-β cell maturation *in vitro* from other research groups.

RESULTS

SIX2 Is Crucial for Acquisition of Glucose-Stimulated Insulin Secretion

Since SIX2 is expressed in human β cells, but its regulatory role during β cell differentiation and maturation is uncharacterized, we measured its gene expression during our 6-stage differentiation protocol (Figure 1A). We observed a notably large increase in
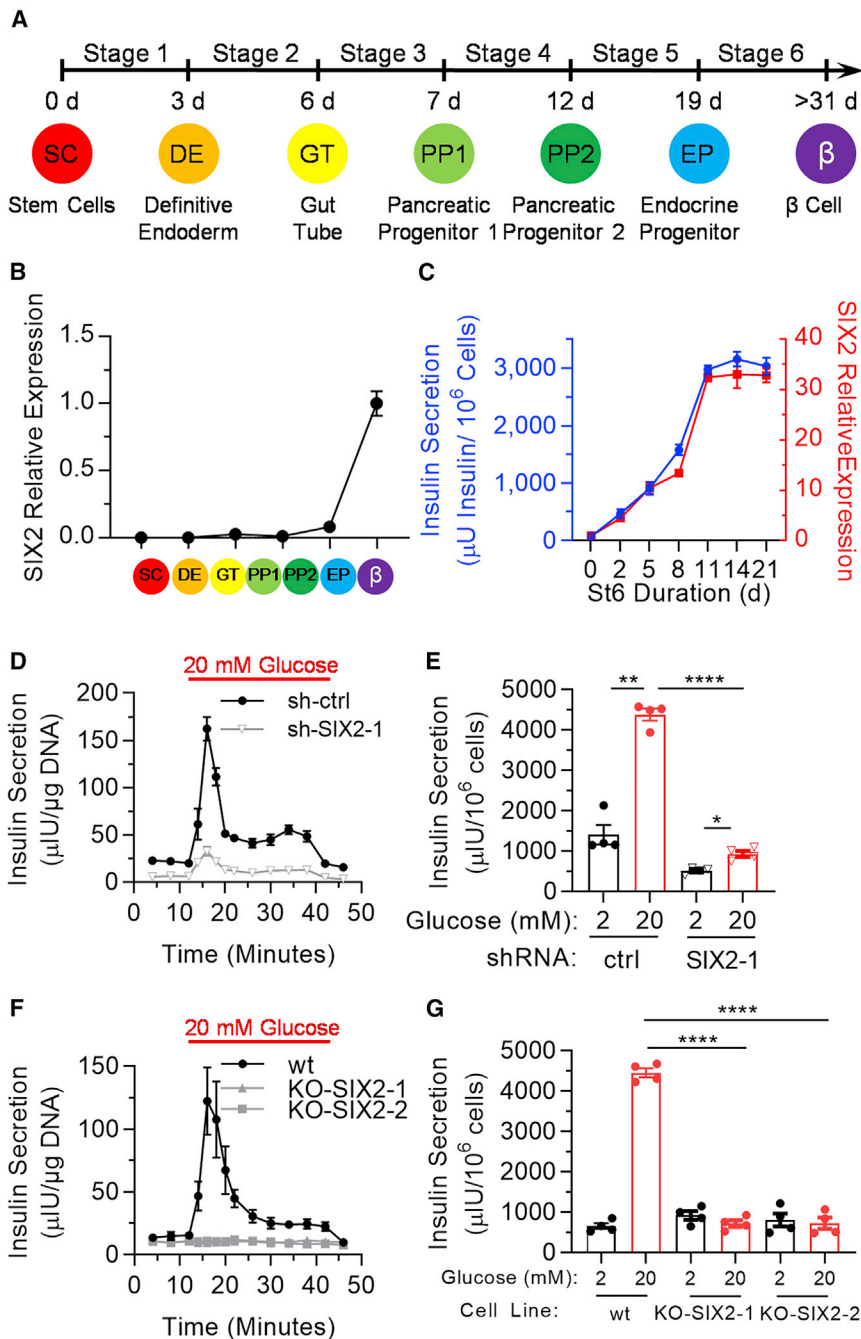
A

B **C**

D **E**

F **G**

Figure 1. SIX2 Controls Glucose-Stimulated Insulin Secretion in Human SC-β Cells

(A) Schematic of hESC differentiation process.

(B) Real-time PCR measurements of SIX2 in un-differentiated hESCs and at the end of each stage of the differentiation. Data are presented as the fold change relative to stage 6 cells. n = 3.

(C) Real-time PCR measurements of SIX2 as a function of time in stage 6 plotted against insulin secretion of sampled cells placed in 20 mM glucose for 1 h. n = 4.

(D) Dynamic glucose-stimulated insulin secretion of stage 6 cells transfected with control shRNA (sh-ctrl; n = 3) or shRNA targeting SIX2 (sh-SIX2-1; n = 4). Cells are perfused with 2 mM glucose, except when indicated, in a perifusion chamber.

(E) Static glucose-stimulated insulin secretion of sh-ctrl or sh-SIX2-1 transduced stage 6 cells. n = 4.

(F) Dynamic glucose-stimulated insulin secretion of wild-type (WT) (n = 4), KO-SIX2-1 (n = 3 technical replicates), or KO-SIX2-2 (n = 3 technical replicates) stage 6 cells.

(G) Static glucose-stimulated insulin secretion of WT, KO-SIX2-1, or KO-SIX2-2 stage 6 cells. n = 4. All data in (B)–(E) were generated with cells from protocol 1 and all data in (F) and (G) were generated with cells from protocol 2.

*p < 0.05, **p < 0.01, ****p < 0.0001 by 2-way paired (for low-high glucose comparison) or unpaired (for high-high glucose comparison) t test. Error bars represent s.e.m.

See also Figure S1.

expression during the maturation of endocrine progenitors to SC-β cells (Figure 1B). Closer inspection of stage 6 revealed that the gene expression of SIX2 increased 32.5 ± 0.9 times during the first 11 days, correlating with increases in insulin protein secretion per cell for the same time period (Figure 1C).

To further study SIX2 using our SC-β cell platform, we generated 2 lentiviruses carrying shRNAs (sh-SIX2-1 and sh-SIX2-2) to KD the expression of SIX2 (Figures S1A and S1B). For these KD studies, we transduced cells on the first day of stage 6 to limit the emergence of SIX2 expression with time. KD of SIX2 in differentiating hESCs (HUES8) and human induced pluripotent stem

cells (hiPSCs) (1013-4FA) lines resulted in significant reductions in both dynamic and static glucose-stimulated insulin secretion assays (Figures 1D, 1E, and S1C–S1F). While peaks in the dynamic insulin secretion profile resembling first- and second-phase insulin secretion were still observed, the overall amount of insulin secreted per DNA was 4.2 ± 1.2 times lower at high glucose with SIX2 KD (Figure 1D). Similarly, for the static assay, while the cells still responded, albeit more weakly, to glucose by secreting elevated insulin, insulin secretion per cell was 4.7 ± 0.8 times lower at high glucose with SIX2 KD (Figure 1E). We do note that the magnitude of the relative insulin secretion at low glucose differed between static and dynamic assays, perhaps due to fluid shear or paracrine effects.

Since the KD studies supported a connection between SIX2 and the acquisition of SC-β cell function, we used CRISPR-Cas9 to KO *SIX2* by deleting the SIX2 coding sequence to create 2 homozygous KO hESC lines (KO-SIX2-1 and KO-SIX-2) to ensure the complete absence of SIX2 (Figures S1G–S1K). Similar to the KD studies, KO of *SIX2* also resulted in significant reductions in both dynamic and static glucose-stimulated insulin secretion assays (Figures 1F and 1G). In contrast to the KD
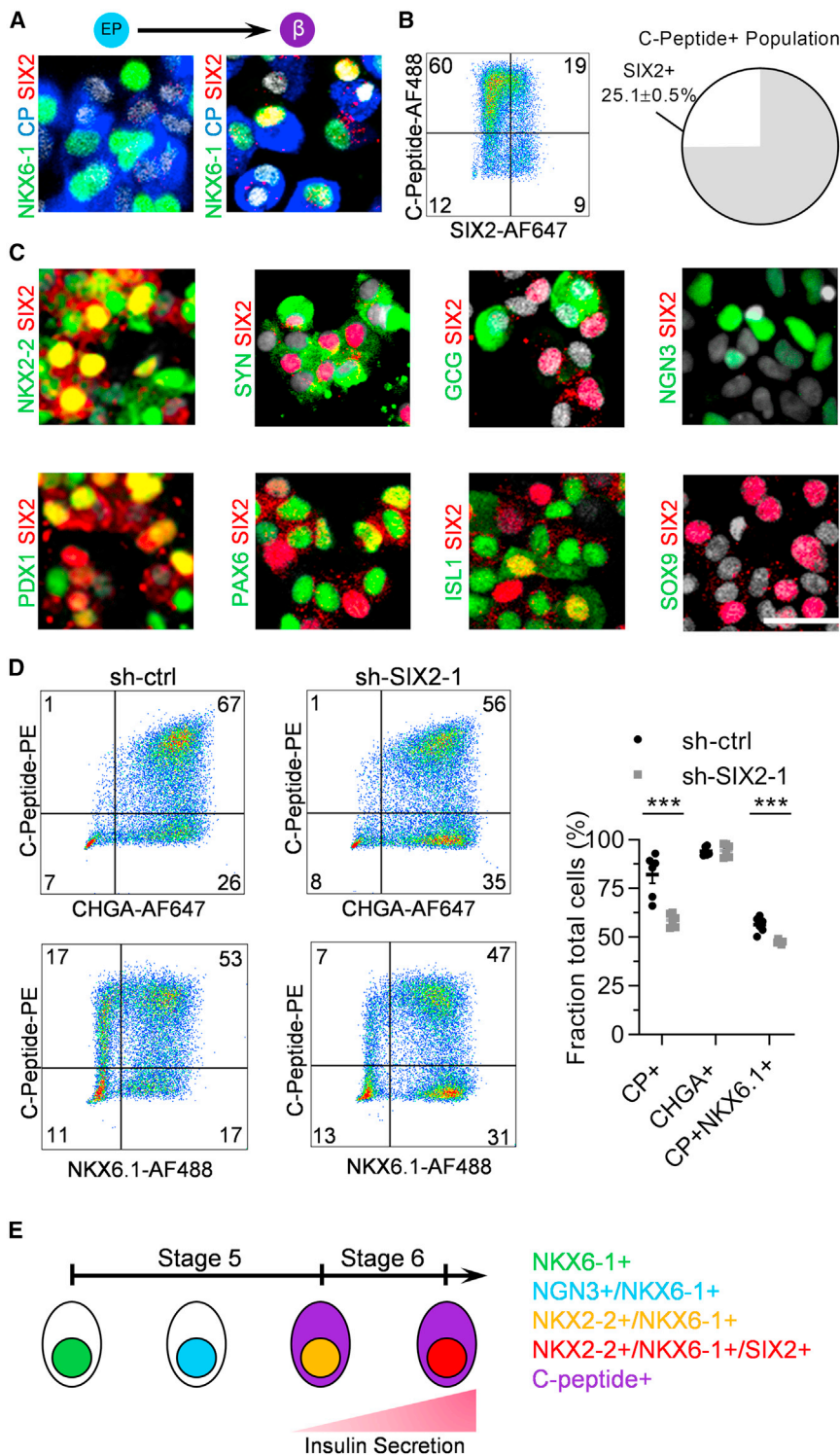
Figure 2. Subtypes of Differentiated Stage 6 Cells Express SIX2

(A) Immunostaining of SIX2 with the β cell markers NKX6-1 and C-peptide at the end of stages 5 (left) and 6 (right).

(B) Flow cytometric quantification of co-expression of C-peptide with SIX2. n = 4.

(C) Immunostaining of SIX2 with a panel of pancreatic markers at the end of stage 6 with the exception of NGN3/SIX2, which was stained 3 days into stage 5.

(D) Flow cytometric quantification of stage 6 cells staining for C-peptide, NKX6.1, and chromogranin A using sh-ctrl and sh-SIX2-1 transduced cells. n = 6. ***p < 0.001 by 2-way unpaired t test.

(E) Schematic summary of marker progression in stages 5 and 6.

Scale bar, 25 μm. Error bars represent s.e.m.

See also Figure S2.

glucose for *SIX2* KO (Figures 1F and 1G). Arda et al. (2016) showed that SIX3, a different transcription factor within the SIX family, is enriched in adult human islets relative to juvenile islets and that its expression is associated with increased β cell function. We measured the expression profile of SIX3 during our SC-β cell differentiation (Figure S2A). While increased expression during early definitive endoderm induction was measured, SIX3 expression was low or undetected at the end of the protocol, and KD or KO of *SIX2* did not alter SIX3 expression (Figure S2B). These data establish SIX2 as a potent regulator of human β cell acquisition of functional maturation *in vitro*, demonstrating that SIX2 is necessary for first- and second-phase insulin secretion in response to glucose. SIX2 is not required for insulin production and secreting, but the lack of SIX2 reduced insulin secretion when cells are exposed to high glucose.

Characterization of SIX2 Expression During SC-β Cell Differentiation

Next, we characterized the expression profile of SIX2 protein throughout the differentiation process. Using immunofluorescence, we did not detect SIX2 expression in C-peptide⁺ cells at the beginning of stage 6, but after 11 days in stage 6, some C-peptide⁺ cells expressed nuclear SIX2 (Figure 2A). Virtually all SIX2⁺ cells co-expressed NKX6-1 (Figure 2A). With flow cytometry, we demonstrated that 25.1% ± 0.5% of the C-peptide⁺ cells co-expressed SIX2 in stage 6 (Figure 2B). However, some SIX2⁺

studies, *SIX2* KO resulted in no first- and second-phase dynamic insulin responses to high glucose and no response to glucose in the static assay. In addition, the overall amount of insulin secreted per DNA was 4.2 ± 0.7 times lower in the dynamic assay and per cell was 6.2 ± 1.5 times lower in the static assay at high

cells were observed outside the C-peptide$^+$ population and are of unknown identity. We also observed that SIX2 was restricted to NKX2-2$^+$ and synaptophysin$^+$ (SYN) cells in stage 6 (Figure 2C), indicating that the expression of SIX2 is restricted to this endocrine cell population. In spite of this, SIX2 was not observed in NGN3$^+$ cells during stage 5 (Figure 2C), even with many of these cells co-expressing NKX6-1 (Figure S2C). Virtually all SIX2$^+$ cells also co-expressed other pancreatic markers, such as ISL1, PAX6, and PDX1 (Figure 2C). Furthermore, the α cell hormone-expressing glucagon$^+$ (GCG) cells did not express SIX2, and SOX9$^+$ progenitors were absent in the stage 6 population (Figure 2C). KD of SIX2 reduced the fraction of cells expressing C-peptide$^+$ and co-expressing C-peptide with NKX6.1 (Figures 2D and S2D), demonstrating an effect on cell fate, while KO of SIX2 did not affect pancreatic progenitors (Figure S2E). These data demonstrate that SIX2 protein expression is only detected in the endocrine population and influences final cell fate.

Transcriptional Profiling of SIX2 KD cells

To further explore the role of SIX2 on SC-β cells, we used RNA sequencing to measure the transcriptome of stage 6 cells transduced with shRNA to KD SIX2 expression. A large number (10,421) of genes were significantly (adjusted p < 0.05) affected by the KD of SIX2, including individual genes associated with β cell function and off-target non-β cell genes (Figures 3 and S3; Table S1). Of the significantly different genes, 633 were enriched in the control cells and 509 were enriched in the SIX2 KD cells by at least a factor of 2 (Figure 3B).

Several gene sets important for β cells, such as those correlated with β cell fate, β cell maturation, exocytosis, potentiation of insulin secretion, and maturation, were controlled by SIX2 (Figures 3C–3E, S3A, andS3B; Tables S2 and S3). The specific established gene sets that are well known included the gene sets β cell enriched (CARTPT, IAPP, GLP1R, GCK, ABCC8, PAX6, INS), calcium signaling (HPCAL4, CAMKK2A, CACNA1S), potassium channels (ATP1A3, KCNN3, KCNMA1), cyclic AMP (cAMP) signaling (ADCY8, CREB5, ADCY3), and protein kinase C (PKC) signaling (PRKC3, PRKCH, PRKCA). In addition, undesirable off-target markers, including liver (ALB, AFP), anterior endoderm (SOX2), and posterior endoderm (CDX2), and gene sets, such as glycolysis, were enriched in the SIX2 KD cells. We validated RNA sequencing results with a subset of relevant genes using real-time PCR in the 1013-4FA hiPSC background (Figure S3C). We compared our RNA sequencing data to recent gene sets identified in Veres et al. (2019) and Nair et al. (2019) as positively correlating with time in the final stage of differentiation of SC-β cells *in vitro*. We found that our SIX2 KD data were statistically associated with the Veres et al. and Nair et al. gene sets (Figures 3C, 3D, S3B, and S4; Table S3). Specifically, the KD of SIX2 repressed many of the genes that increased expression in Veres et al. (2019) and Nair et al. (2019), suggesting that many of these identified genes are controlled by SIX2. These data support the conclusion that SIX2 controls the expression of many β cell genes related to normal physiological function and differentiation.

Physiological Profiling of SIX2 KD SC-β Cells

We followed up on key β cell processes implicated by the SIX2 KD RNA sequencing data. First, we found that KD of SIX2

reduced insulin content and INS gene expression, but it did not affect insulin processing (Figures 4A–4C and S4A). Second, we assessed mitochondrial respiration and glycolysis because switching from glycolysis to mitochondrial respiration is necessary for the maturation and normal physiological function of β cells (Nair et al., 2019). The Seahorse XFe24 extracellular flux assay was used to measure the oxygen consumption rate (OCR) and the extracellular acidification rate (ECAR), respectively. KD of SIX2 resulted in a decreased OCR and ratio of OCR to ECAR (Figures 4D, 4E, and S4C). Cytoplasmic calcium flux was also evaluated, as the influx of calcium is necessary before insulin secretion and is triggered by glucose-induced depolarization in β cells (Rutter and Hodson, 2013). KD of SIX2 slightly decreased glucose-stimulated and greatly decreased KCl-stimulated increases in cytoplasmic calcium as determined with Fluo-4 AM stained cells (Figure 4F). These data are consistent with decreased glucose-stimulated insulin secretion (Figures 1D–1G and S1C–S1F) and the RNA sequencing analysis (Figure 3), indicating that SIX2 plays a key role in the metabolism and upstream signaling relating to the functional maturation of SC-β cells.

Finally, we explored other known insulin secretagogues, observing that while SIX2 KD cells were able to respond to all treatments, the amount of insulin secretion was much lower than the control (Figure 4G). Stimulation with KCl and 3-isobutyl-1-methylxanthine (IBMX) demonstrated that SIX2 KD cells were capable of elevating insulin secretion, but glucose-dependent secretion was severely impaired without SIX2. Furthermore, considering the large amount of insulin secretion with treatments targeting downstream processes, particularly depolarization (KCl) and cAMP accumulation (IBMX), upstream mechanisms appear more affected by SIX2 KD, namely glucose sensing and metabolism. In addition to defects in glucose-stimulated insulin secretion, SC-β cells with KD of SIX2 have defects in insulin content, mitochondrial respiration, calcium signaling, and response to a wide array of secretagogues.

DISCUSSION

Here, we demonstrate that SIX2 influences the generation human SC-β cells *in vitro*. Increases in SIX2 expression correlates with increases in insulin secretion as SC-β cells mature during stage 6 of the differentiation protocols. KD or KO of SIX2 dramatically reduces glucose-stimulated insulin secretion, including first- and second-phase dynamic insulin release and the total amount of insulin released from the cells. Expression of SIX2 protein appears to be restricted to endocrine cells. RNA sequencing of cells with the KD of SIX2 reveals that a large number of gene sets associated with β cells and off-targets are negatively affected, including recently defined gene sets of maturing SC-β cells. We confirmed the physiological effects of many of these gene sets by measuring reductions in insulin content, insulin gene expression, mitochondrial respiration, calcium flux, and insulin secretion in response to compounds that block the K^{ATP} channel (tolbutamide), accumulate cAMP (IBMX), activate GLP1R (Exendin-4), and depolarize the membrane (KCl).

A major goal in regenerative medicine is to generate fully mature replacement cells differentiated from stem cells.
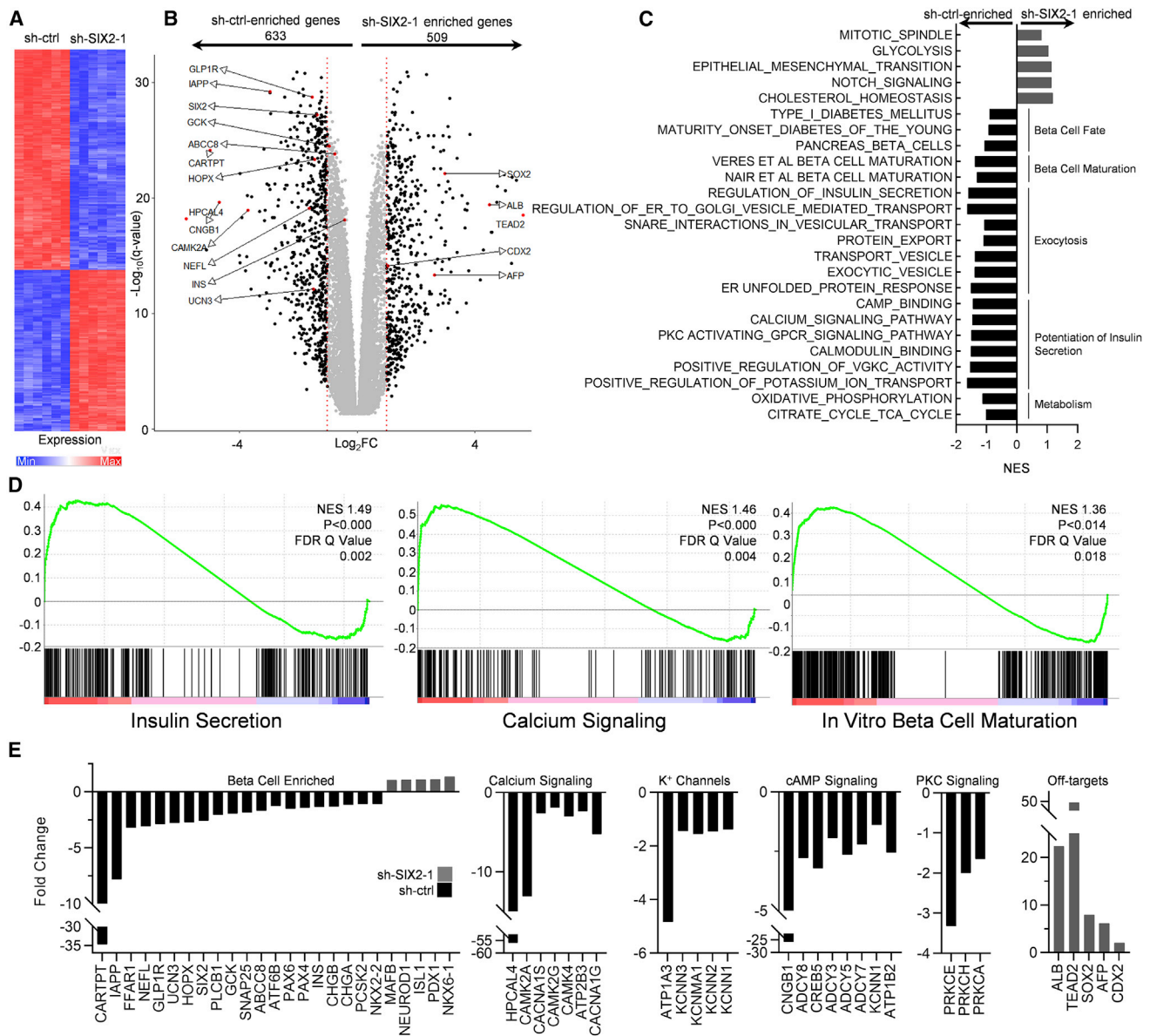
Figure 3. SIX2 Regulates Important β Cell Genes and Gene Sets

(A) Heatmap of 1,000 most differentially expressed genes between stage 6 cells transduced with sh-ctrl and sh-SIX2-1 by p value. n = 6.

(B) Volcano plot showing all differentially expressed genes. Genes with at least a 2-fold change (FC) are in black. Genes of particular interest are highlighted.

(C) Selected enriched gene sets for important β cell processes from the Molecular Signatures Database. Also included 2 custom gene sets comprising 76 genes identified in Veres et al. (2019) and the top 424 genes identified in Nair et al. (2019) positively correlating with time and maturation *in vitro*. NES, normalized enrichment score.

(D) Enrichment plots from the shown gene sets.

(E) FCs from genes within enriched β cell-related gene sets.

See also Figure S3 and Tables S1–S3.

However, while many differences often exist in the function and gene expression of stem cell-differentiated cells, often referred to as the maturation phenotype specific to the differentiated cells in question, identifying specific parameters on which to focus is often difficult due to a lack of understanding of human developmental biology. In the case of SC-β cells, many genes and pathways have been focused on and studied in the context of

improving these cells, including YAP (Rosado-Olivieri et al., 2019), the ROCKII pathway (Ghazizadeh et al., 2017), the transforming growth factor β (TGF-β) pathway (Velazco-Cruz et al., 2019), and the cytoskeleton (Hogrebe et al., 2020). Further studies have connected diabetic pathogenetic variants with impairments in polyhormonal endocrine or SC-β cells, including INS (Balboa et al., 2018; Ma et al., 2018), HNF1-α
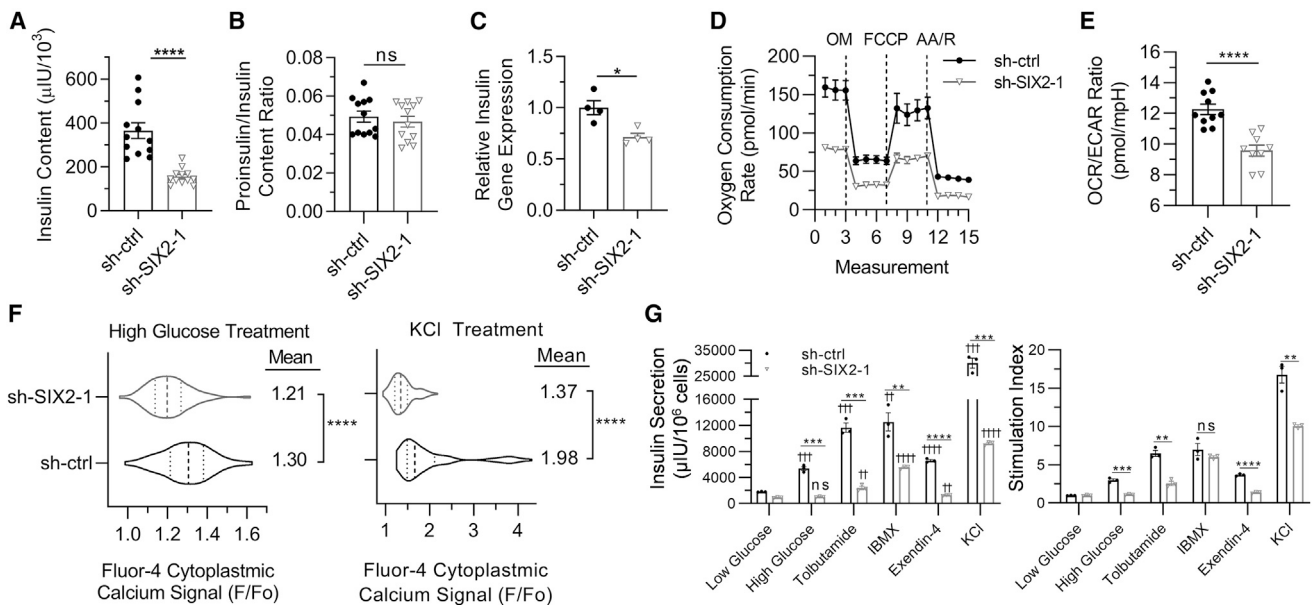
Figure 4. SIX2 Affects Insulin Content, Mitochondrial Respiration, Cytoplasmic Calcium Flux, and Response to Secretagogues in SC-β cells

(A) Insulin content for stage 6 cells. n = 12. ****$p < 0.0001$ by 2-way unpaired t test.

(B) Proinsulin:insulin content ratio for stage 6 cells. n = 12. ns (non-significant) by 2-way unpaired t test.

(C) Real-time PCR measurements of INS gene expression for stage 6 cells. n = 4. *$p < 0.05$ by 2-way unpaired t test.

(D) OCR measurements under basal conditions and after sequential injections of oligomycin (OM), carbonyl cyanide-4-(trifluoromethoxy)phenylhydrazone (FCCP), and antimycin A with rotenone (AA/R). n = 10 for sh-ctrl and n = 9 for sh-SIX2-1.

(E) Calculated OCR:ECAR ratio under basal conditions. n = 10 for sh-ctrl and n = 9 for sh-SIX2-1. ****$p < 0.0001$ by 2-way unpaired t test.

(F) Cytosolic calcium signaling in response to high glucose (20 mM) and high KCl (30 mM) treatment relative to low glucose (2 mM, Fo) for Fluo-4 AM. Violin plots show distribution of cellular responses for sh-ctrl (n = 232) and sh-SIX2-1 (n = 276) transduced cells with median and quartiles marked with dashed lines. ****$p < 0.0001$ by 2-way unpaired t test.

(G) Static glucose-stimulated insulin secretion with cells with 2 mM glucose, 20 mM glucose, or 20 mM glucose with the indicated compound. n = 3. ns, ** or ††$p < 0.01$, *** or †††$p < 0.001$, **** or ††††$p < 0.0001$ by 2-way unpaired t test. * indicates comparison within same compound treatment. † indicates comparison with low glucose with same shRNA treatment.

Error bars represent s.e.m.

See also Figure S4.

(Cardenas-Diaz et al., 2019), WFS1 (Maxwell et al., 2020; Shang et al., 2014), ZNT8 (Dwivedi et al., 2019), NEUROD1 (Romer et al., 2019), and GCK (Hua et al., 2013).

In contrast, here, we focus on the role of SIX2 in the differentiation to and maturation of SC-β cells and establish a critical connection between this transcription factor and the generation and functional maturation of SC-β cells, particularly regarding glucose-stimulated insulin secretion. Arda et al. (2016) studied both SIX2 and SIX3 in the human insulinoma EndoC-βH1 cell line and found overexpressing SIX3 but not SIX2 to increase insulin secretion and content in addition to increased expression of these genes in adult versus juvenile islets, supporting differing roles for these transcription factors. Our study differs from that of Arda et al. (2016) in several respects. We studied SIX2 in the context of differentiating and maturing SC-β cells, the process of which has increasing SIX2 expression as cells mature with time, a considerably different developmental context than that modeled by EndoC-βH1 cells. Furthermore, our study investigates many other aspects of β cell phenotype not explored by Arda et al., including demonstrating that both first- and second-phase dynamic insulin secretion are eliminated with KO of *SIX2*, made possible by our recent discoveries of generating

SC-β cells using these functional characterizations (Velazco-Cruz et al., 2019), indexing transcriptional changes with KD of SIX2, and showing how mechanisms of β cell glucose sensing, respiration, and calcium flux are disrupted with KD of SIX2. Furthermore, while our data demonstrate the importance of SIX2 in SC-β cells, this transcription factor is in the presence of many other transcription factors that are important for the β cell phenotype, including PDX1, NKX6-1, NKX2-2, and NEUROD1 (Hogrebe et al., 2020). Understanding the molecular interactions and regulatory network of SIX2 with these transcription factors would be valuable in future studies.

Differences in transcriptional regulation in rodent and human β cells are well known (Benner et al., 2014). Since SIX2 expression is restricted to human β cells (Segerstolpe et al., 2016; Xin et al., 2016), focused studies on human cell model systems, such as that provided by our *in vitro* differentiation platform, are essential in the investigation of cell maturation and disease. Proper understanding of the molecular mechanisms that control human β cell maturation is necessary for developing further improvements in SC-β cell technologies for diabetes cell-replacement therapies. As only a fraction of C-peptide+ cells currently express SIX2 in our study, increased co-expression could result in differentiated

populations with increased function and utility for cell therapy. Further study into the role of SIX2 could reveal new insights into increasing the functional maturation of SC-β cells and the regulation of expression of other β cell genes, such as MAFA (Nair et al., 2019; Velazco-Cruz et al., 2019), or β cell failure in type 2 diabetes.

STAR★METHODS

Detailed methods are provided in the online version of this paper and include the following:

- KEY RESOURCES TABLE
- RESOURCE AVAILABILITY
  - Lead Contact
  - Materials Availability
  - Data and Code Availability
- EXPERIMENTAL MODEL AND SUBJECT DETAILS
  - Culture of undifferentiated hESCs and differentiation to Stage 6 cells
- METHOD DETAILS
  - Real-time PCR
  - KD of SIX2
  - Generation of SIX2 KO cell lines
  - Static glucose-stimulated insulin secretion
  - Dynamic glucose-stimulated insulin secretion
  - Immunostaining
  - Flow cytometry
  - RNA sequencing
  - Hormone content measurements
  - OCR and ECAR measurements
  - Cytoplasmic calcium measurements
- QUANTIFICATION AND STATISTICAL ANALYSIS

SUPPLEMENTAL INFORMATION

Supplemental Information can be found online at https://doi.org/10.1016/j.celrep.2020.107687.

AUTHOR CONTRIBUTIONS

L.V.-C. and J.R.M. conceived of the experimental design. All of the authors contributed to the experimentation. L.V.C. and J.R.M. wrote the manuscript, which was reviewed and edited by all of the authors.

REFERENCES

Arda, H.E.E., Li, L., Tsai, J., Torre, E.A.A., Rosli, Y., Peiris, H., Spitale, R.C.C., Dai, C., Gu, X., Qu, K., et al. (2016). Age-Dependent Pancreatic Gene Regulation Reveals Mechanisms Governing Human β Cell Function. Cell Metab. *23*, 909–920.

Balboa, D., Saarimäki-Vire, J., Borshagovski, D., Survila, M., Lindholm, P., Galli, E., Eurola, S., Ustinov, J., Grym, H., Huopio, H., et al. (2018). Insulin mutations impair beta-cell development in a patient-derived iPSC model of neonatal diabetes. eLife *7*, e38519.

Bellin, M.D., Barton, F.B., Heitman, A., Harmon, J.V., Kandaswamy, R., Balamurugan, A.N., Sutherland, D.E.R., Alejandro, R., and Hering, B.J. (2012). Potent induction immunotherapy promotes long-term insulin independence after islet transplantation in type 1 diabetes. Am. J. Transplant. *12*, 1576–1583.

Benner, C., van der Meulen, T., Cacéres, E., Tigyi, K., Donaldson, C.J., and Huising, M.O. (2014). The transcriptional landscape of mouse beta cells compared to human beta cells reveals notable species differences in long non-coding RNA and protein-coding gene expression. BMC Genomics *15*, 620.

Cardenas-Diaz, F.L., Osorio-Quintero, C., Diaz-Miranda, M.A., Kishore, S., Leavens, K., Jobaliya, C., Stanescu, D., Ortiz-Gonzalez, X., Yoon, C., Chen, C.S., et al. (2019). Modeling Monogenic Diabetes using Human ESCs Reveals Developmental and Metabolic Deficiencies Caused by Mutations in HNF1A. Cell Stem Cell *25*, 273–289.e5.

D'Amour, K.A., Agulnick, A.D., Eliazer, S., Kelly, O.G., Kroon, E., and Baetge, E.E. (2005). Efficient differentiation of human embryonic stem cells to definitive endoderm. Nat. Biotechnol. *23*, 1534–1541.

D'Amour, K.A., Bang, A.G., Eliazer, S., Kelly, O.G., Agulnick, A.D., Smart, N.G., Moorman, M.A., Kroon, E., Carpenter, M.K., and Baetge, E.E. (2006). Production of pancreatic hormone-expressing endocrine cells from human embryonic stem cells. Nat. Biotechnol. *24*, 1392–1401.

Dwivedi, O.P., Lehtovirta, M., Hastoy, B., Chandra, V., Krentz, N.A.J., Kleiner, S., Jain, D., Richard, A.-M., Abaitua, F., Beer, N.L., et al. (2019). Loss of ZnT8 function protects against diabetes by enhanced insulin secretion. Nat. Genet. *51*, 1596–1606.

Ghazizadeh, Z., Kao, D.I., Amin, S., Cook, B., Rao, S., Zhou, T., Zhang, T., Xiang, Z., Kenyon, R., Kaymakcalan, O., et al. (2017). ROCKII inhibition promotes the maturation of human pancreatic beta-like cells. Nat. Commun. *8*, 298.

Gu, G., Dubauskaite, J., and Melton, D.A. (2002). Direct evidence for the pancreatic lineage: NGN3+ cells are islet progenitors and are distinct from duct progenitors. Development *129*, 2447–2457.

Hachiya, T., Komaki, S., Hasegawa, Y., Ohmomo, H., Tanno, K., Hozawa, A., Tamiya, G., Yamamoto, M., Ogasawara, K., Nakamura, M., et al. (2017). Genome-wide meta-analysis in Japanese populations identifies novel variants at the TMC6-TMC8 and SIX3-SIX2 loci associated with HbA1c. Sci. Rep. *7*, 16147.

Hogrebe, N.J., Augsornworawat, P., Maxwell, K.G., Velazco-Cruz, L., and Millman, J.R. (2020). Targeting the cytoskeleton to direct pancreatic differentiation of human pluripotent stem cells. Nat. Biotechnol. *38*, 460–470.

Hua, H., Shang, L., Martinez, H., Freeby, M., Gallagher, M.P., Ludwig, T., Deng, L., Greenberg, E., Leduc, C., Chung, W.K., et al. (2013). iPSC-derived β cells model diabetes due to glucokinase deficiency. J. Clin. Invest. *123*, 3146–3153.

Kenty, J.H., and Melton, D.A. (2015). Testing pancreatic islet function at the single cell level by calcium influx with associated marker expression. PLoS One 10, e0122044.

Kim, Y.J., Go, M.J., Hu, C., Hong, C.B., Kim, Y.K., Lee, J.Y., Hwang, J.-Y., Oh, J.H., Kim, D.-J., Kim, N.H., et al.; MAGIC Consortium (2011). Large-scale genome-wide association studies in East Asians identify new genetic loci influencing metabolic traits. Nat. Genet. 43, 990–995.

Ma, S., Viola, R., Sui, L., Cherubini, V., Barbetti, F., and Egli, D. (2018). β Cell Replacement after Gene Editing of a Neonatal Diabetes-Causing Mutation at the Insulin Locus. Stem Cell Reports 11, 1407–1415.

Maxwell, K.G., Augsornworawat, P., Velazco-Cruz, L., Kim, M.H., Asada, R., Hogrebe, N.J., Morikawa, S., Urano, F., and Millman, J.R. (2020). Gene-edited human stem cell–derived β cells from a patient with monogenic diabetes reverse preexisting diabetes in mice. Sci. Transl. Med. 12, eaax9106.

McCall, M., and Shapiro, A.M.J. (2012). Update on islet transplantation. Cold Spring Harb. Perspect. Med. 2, a007823.

Millman, J.R., and Pagliuca, F.W. (2017). Autologous Pluripotent Stem Cell-Derived β-Like Cells for Diabetes Cellular Therapy. Diabetes 66, 1111–1120.

Millman, J.R., Xie, C., Van Dervort, A., Gürtler, M., Pagliuca, F.W., and Melton, D.A. (2016). Generation of stem cell-derived β-cells from patients with type 1 diabetes. Nat. Commun. 7, 11463.

Millman, J.R., Doggett, T., Thebeau, C., Zhang, S., Semenkovich, C.F., and Rajagopal, R. (2019). Measurement of Energy Metabolism in Explanted Retinal Tissue Using Extracellular Flux Analysis. J. Vis. Exp. (143) https://doi.org/10.3791/58626.

Nair, G.G., Liu, J.S., Russ, H.A., Tran, S., Saxton, M.S., Chen, R., Juang, C., Li, M.L., Nguyen, V.Q., Giacometti, S., et al. (2019). Recapitulating endocrine cell clustering in culture promotes maturation of human stem-cell-derived β cells. Nat. Cell Biol. 21, 263–274.

Pagliuca, F.W., Millman, J.R., Gürtler, M., Segel, M., Van Dervort, A., Ryu, J.H., Peterson, Q.P., Greiner, D., and Melton, D.A. (2014). Generation of functional human pancreatic β cells in vitro. Cell 159, 428–439.

Rezania, A., Bruin, J.E., Arora, P., Rubin, A., Batushansky, I., Asadi, A., O'Dwyer, S., Quiskamp, N., Mojibian, M., Albrecht, T., et al. (2014). Reversal of diabetes with insulin-producing cells derived in vitro from human pluripotent stem cells. Nat. Biotechnol. 32, 1121–1133.

Romer, A.I., Singer, R.A., Sui, L., Egli, D., and Sussel, L. (2019). Murine Perinatal β-Cell Proliferation and the Differentiation of Human Stem Cell-Derived Insulin-Expressing Cells Require NEUROD1. Diabetes 68, 2259–2271.

Rosado-Olivieri, E.A., Anderson, K., Kenty, J.H., and Melton, D.A. (2019). YAP inhibition enhances the differentiation of functional stem cell-derived insulin-producing β cells. Nat. Commun. 10, 1464.

Rutter, G.A., and Hodson, D.J. (2013). Minireview: intraislet regulation of insulin secretion in humans. Mol. Endocrinol. 27, 1984–1995.

Segerstolpe, Å., Palasantza, A., Eliasson, P., Andersson, E.-M., Andréasson, A.-C., Sun, X., Picelli, S., Sabirsh, A., Clausen, M., Bjursell, M.K., et al. (2016). Single-Cell Transcriptome Profiling of Human Pancreatic Islets in Health and Type 2 Diabetes. Cell Metab. 24, 593–607.

Shang, L., Hua, H., Foo, K., Martinez, H., Watanabe, K., Zimmer, M., Kahler, D.J., Freeby, M., Chung, W., LeDuc, C., et al. (2014). β-Cell dysfunction due to increased ER stress in a stem cell model of Wolfram syndrome. Diabetes 63, 923–933.

Spracklen, C.N., Shi, J., Vadlamudi, S., Wu, Y., Zou, M., Raulerson, C.K., Davis, J.P., Zeynalzadeh, M., Jackson, K., Yuan, W., et al. (2018). Identification and functional analysis of glycemic trait loci in the China Health and Nutrition Survey. PLoS Genet. 14, e1007275.

Subramanian, A., Tamayo, P., Mootha, V.K., Mukherjee, S., Ebert, B.L., Gillette, M.A., Paulovich, A., Pomeroy, S.L., Golub, T.R., Lander, E.S., et al. (2005). Gene set enrichment analysis: a knowledge-based approach for interpreting genome-wide expression profiles. Proc. Natl. Acad. Sci. USA 102, 15545–15550.

Velazco-Cruz, L., Song, J., Maxwell, K.G., Goedegebuure, M.M., Augsornworawat, P., Hogrebe, N.J., and Millman, J.R. (2019). Acquisition of Dynamic Function in Human Stem Cell-Derived β Cells. Stem Cell Reports 12, 351–365.

Veres, A., Faust, A.L., Bushnell, H.L., Engquist, E.N., Kenty, J.H., Harb, G., Poh, Y.C., Sintov, E., Gürtler, M., Pagliuca, F.W., et al. (2019). Charting cellular identity during human in vitro β-cell differentiation. Nature 569, 368–373.

Xin, Y., Kim, J., Okamoto, H., Ni, M., Wei, Y., Adler, C., Murphy, A.J., Yancopoulos, G.D., Lin, C., and Gromada, J. (2016). RNA Sequencing of Single Human Islet Cells Reveals Type 2 Diabetes Genes. Cell Metab. 24, 608–615.

Cell Reports
Report

STAR★METHODS

KEY RESOURCES TABLE

REAGENT or RESOURCE	SOURCE	IDENTIFIER
Antibodies		
Rat anti C-peptide	DSHB	Cat#GN-ID4; RRID:AB_2255626
Mouse anti NKX6-1	DSHB	Cat#F55A12; RRID:AB_532379
Mouse anti Glucagon	ABCAM	Cat#ab82270; RRID:AB_1658481
Goat anti PDX1	R&D Systems	Cat#AF2419; RRID:AB_355257
Mouse anti PAX6	BDBiosciences	Cat#561462; RRID:AB_10715442
Rabbit anti CHGA	ABCAM	Cat#ab15160
Mouse anti ISL1	DSHB	Cat#40.2D6; RRID:AB_528315
Rabbit anti SIX2	Proteintech	Cat#11562-1-AP; RRID:AB_2189084
Sheep anti NGN3	R&D Systems	Cat#AF3444; RRID:AB_2149527
Mouse anti NKX2-2	DSHB	Cat#74.5A5; RRID:AB_531794
Mouse anti Synaptophysin	LifeSpan BioSciences	Cat#LS-C174787; RRID:AB_2811021
Mouse anti SOX9	Invitrogen	Cat#14-9765-80; RRID:AB_2573005
anti-rat-alexa fluor 488	Invitrogen	Cat#A-21208; RRID:AB_141709
anti-mouse-alexa fluor 647	Invitrogen	Cat#a31571; RRID:AB_162542
anti-rabbit-alexa fluor 647	Invitrogen	Cat#a31573; RRID:AB_2536183
anti-goat-alexa fluor 647	Invitrogen	Cat#a21447; RRID:AB_141844
anti-rabbit-alexa fluor 488	Invitrogen	Cat#a21206; RRID:AB_2535792
anti-mouse-alexa fluor 594	Invitrogen	Cat#a21203; RRID:AB_141633
anti-rabbit-alexa fluor 594	Invitrogen	Cat#a21207; RRID:AB_141637
anti-goat-alexa fluor 594	Invitrogen	Cat#a11058; RRID:AB_2534105
anti-rat-PE	Jackson Immuneresearch	Cat#712-116-153; RRID:AB_2340657
anit-sheep-alexa fluor 594	Invitrogen	Cat#a11016; RRID:AB_10562537
Chemicals, Peptides, and Recombinant Proteins		
Lenti-X concentrator	Takara	Cat#631232
mTeSR1	StemCell Technologies	Cat#05850
Accutase	StemCell Technologies	Cat#07920
Y27632	Abcam	Cat#ab120129
Matrigel	Corning	Cat#356230
TrypLE	Life Technologies	Cat#12-604-039
Dnase	QIAGEN	Cat#79254
HEPES	GIBCO	Cat#15630-080
Extendin-4	MilliporeSigma	Cat#E7144
IBMX	MilliporeSigma	Cat#I5879
Tolbutamide	MilliporeSigma	Cat#T0891
KCl	ThermoFisher	Cat#BP366500
Tris	MilliporeSigma	Cat#T6066
EDTA	Ambion	Cat#327371000
Paraformaldehyde	Electron Microscopy Science	Cat#15714
Donkey Serum	Jackson Immunoresearch	Cat#017-000-121
Triton X-100	Acros Organics	Cat#327371000
RPMI-1640	Sigma	Cat#R6504
Oligomycin	Calbiochem	Cat#1404-19-9
FCCP	Sigma	Cat#270-86-5

(Continued on next page)

Continued

REAGENT or RESOURCE	SOURCE	IDENTIFIER
Rotenone	Calbiochem	Cat#83-79-4
Antimycin A	Sigma	Cat#1397-94-0
Fluo-4 AM	Invitrogen	Cat#F14201
DMEM	MilliporeSigma	Cat#D6429
HI Fetal Bovine Serum	MilliporeSigma	Cat#F4135
Opti-MEM	Life Technologies	Cat#31985-070
Polyethylenimine 'Max' MW 40,000 Da	Polysciences	Cat#24765-2
Critical Commercial Assays		
Human Insulin Elisa	ALPCO	Cat#80-INSHU-E10.1; RRID:AB_2801438
Proinsulin ELISA	Mercodia	Cat#10-1118-01; RRID:AB_2754550
Quant-iT Picogreen dsDNA assay kit	MilliporeSigma	Cat#T6066
Lenti-X qRT-PCR Titration Kit	Takara	Cat#631235
RNeasy Mini Kit	QIAGEN	Cat#74016
High Capacity cDNA Reverse Transcriptase Kit	Applied Biosystems	Cat#4368814
PowerUp SYBR Green Master Mix	Applied Biosystems	Cat#A25741
Deposited Data		
Raw and Analyzed RNA Seq Data	This Paper	GEO: GSE147737
Experimental Models: Cell Lines		
Human: HUES8 hESC	HSCI	hES Cell line: HUES-8
Human: iPSC 1013	HSCI	hiPS Cell line: 1013-4FA
Lenti-X 293T	Takara	Cat#632180
Oligonucleotides		
See Table S4.	N/A	N/A
Recombinant DNA		
sh-ctrl	RNAi Core, Washington University in St. Louis	pLKO.1 shGFP, GCGCGATCACATGGTCCTGCT
sh-SIX2-1	RNAi Core, Washington University in St. Louis	pLKO.1 TRC sh-SIX2, CAACGAGAACTCCAATTCTAA
sh-SIX2-2	RNAi Core, Washington University in St. Louis	pLKO.1 TRC sh-SIX2, GAGCACCTTCACAAGAATGAA
psPAX2	Gift from Didier Trono	Addgene Plasmid Cat#12260; RRID:Addgene_12260; http://n2t.net/addgene:12260
pMD2.G	Gift from Didier Trono	Addgene Plasmid Cat#12259; RRID:Addgene_12259; http://n2t.net/addgene:12259
Software and Algorithms		
Fiji ImageJ	ImageJ public freeware	https://imagej.net/Fiji/Downloads
PRISM8	GraphPad	https://www.graphpad.com/scientific-software/prism/
FLOWJO	FLOWJO	https://www.flowjo.com/solutions/flowjo/downloads
GSEA	GSEA	https://www.gsea-msigdb.org/gsea/index.jsp
Other		
30-mL spinner flasks	Reprocell	Cat#ABBWVS03A
Vi-Cell XR	Beckman Coulter	Cat#Vi-Cell XR
Tanswells	Corning	Cat#431752
Seahorse Xfe24 Flux analyzer	Agilent	Cat#Xfe24
#1.5 glass bottom 96 well plate	Cellvis	Cat#963-1.5H-N
8-channel peristaltic pump	ISMATEC	Cat#ISM931C
Inlet/outlet two-stop tubing	ISMATEC	Cat#070602-04i-ND
Cell chamber	BioRep	Cat#Peri-Chamber

Continued

REAGENT or RESOURCE	SOURCE	IDENTIFIER
Dispensing nozzle	BioRep	Cat#Peri-Nozzle
Connection tubbing	BioRep	Cat#Peri-TUB-040
Bio-Gel P-4	Bio-Rad	Cat#150-4124

RESOURCE AVAILABILITY

Lead Contact
Further information and requests for resources and reagents should be directed to and will be fulfilled by the Lead Contact, Jeffrey R. Milman (jmillman@wustl.edu).

Materials Availability
shRNA plasmids used in this study are from the TRC shRNA library and available from the RNAi Core at Washington University in St. Louis.

HUES8 cell line is available through the Harvard Stem Cell Institute (HCSI).

SIX2 KO cell lines are made available upon request to Lead Contact.

Data and Code Availability
The RNA sequencing data generated in this study is made available at the Gene Expression Omnibus (GEO). The accession number for the raw and processed data reported in this paper is GEO: GSE147737.

EXPERIMENTAL MODEL AND SUBJECT DETAILS

Culture of undifferentiated hESCs and differentiation to Stage 6 cells
Cell culture was performed as we previously described (Hogrebe et al., 2020; Millman et al., 2016; Velazco-Cruz et al., 2019). This work was performed with the approval of the Washington University School of Medicine Embryonic Stem Cell Research Oversight Committee (ESCRO). The HUES8 hESC and 1013-4FA hiPSC lines was generously provided by Dr. Douglas Melton (Harvard University) and has been published on previously (Hogrebe et al., 2020; Velazco-Cruz et al., 2019). All data is with the HUES8 cell line unless otherwise noted to be 1013-4FA. For differentiation protocol 1 (Velazco-Cruz et al., 2019), which was used unless otherwise noted, undifferentiated HUES8 were cultured in mTeSR1 (StemCell Technologies; 05850) in 30-mL spinner flasks (REPROCELL; ABBWVS03A) on a rotator stir plate (Chemglass) at 60 RPM in a humidified 37°C 5% CO2 tissue culture incubator. Stem cells were passaged every 3 days by single cell dispersion using Accutase (StemCell Technologies; 07920), viable cells counted with Vi-Cell XR (Beckman Coulter), and seeded at 6×10^5 cells/mL in mTeSR1+ 10 μM Y27632 (Abcam; ab120129). The media was then changed as outlined in Table S4 to induce differentiation. For differentiation protocol 2 (Hogrebe et al., 2020), which was used for the KO studies and 1013-4FA differentiations, undifferentiated pluripotent stem cells were cultured in mTeSR1 on plates coated with Matrigel (Corning; 356230) in a humidified 37°C 5% CO2 tissue culture incubator. Stem cells were passaged every 4 days single cell dispersion using TrypLE (Life Technologies; 12-604-039), viable cells counted with Vi-Cell XR, and seeded at 5.2×10^5 cells/cm^2 in mTeSR1+ 10 μM Y27632. The media was then changed as outlined in Table S4 to induce differentiation. On stage 6 day 1 of protocol 1 and stage 6 day 7 of protocol 2 cells were single cell dispersed using TrypLE (Life Technologies; 12-604-039; 15-minute incubation for protocol 1, 6-minute incubation for protocol 2). Following single cell dispersion cells were re-aggregated by seeding 5 million cells in 5 mL of stage 6 media into a well of a 6-well plate placed on an orbi-shaker (Benchmark) rotating at 100 RPM; clusters were allowed to re-aggregate and media was changed 48 hours post seeding.

METHOD DETAILS

Real-time PCR
Measurements were performed as we previously described (Velazco-Cruz et al., 2019). RNeasy Mini Kit (QIAGEN; 74016) with DNase treatment (QIAGEN; 79254) was used for RNA extraction. High Capacity cDNA Reverse Transcriptase Kit (Applied Biosystems; 4368814) was used to make cDNA. PowerUp SYBR Green Master Mix (Applied Biosystems; A25741) on a StepOnePlus (Applied Biosystems) was used to perform the real-time PCR reactions. Melting curves were ran for each primer to determine specificity of amplification. ΔΔCt methodology with TBP normalization was used for analysis. For samples undetected using real-time PCR CT values where set to 40 in analysis. Primer sequences used were (gene, forward primer, reverse primer): INS, CAATGC CACGCTTCTGC, TTCTACACACCCAAGACCCG; TBP, GCCATAAGGCATCATTGGAC, AACAACAGCCTGCCACCTTA; SIX2, AAGGCACACTACATCGAGGC, CACGCTGCGACTCTTTTCC; SIX3, CTGCCCACCCTCAACTTCTC, GCAGGATCGACTC GTGTTTGT; IAPP, ACATGTGGCAGTGTTGCATT, TCATTGTGCTCTCTGTTGCAT; UCN3, TGTAGAACTTGTGGGGGAGG,

GGAGGGAAGTCCACTCTCG; <u>ABCC8</u>, GCCCACGAAAGTTATGAGGA, AAGGAGATGACCAGCCTCAG; <u>GCK</u>, ATGCTGGACGACA GAGCC, CCTTCTTCAGGTCCTCCTCC; <u>GLP1R1</u>, GGTGCAGAAATGGCGAGAATA, CCGGTTGCAGAACAAGTCTGT; <u>HOPX,</u> GA GACCCAGGGTAGTGATTTGA, AAAAGTAATCGAAAGCCAAGCAC; <u>NEFL</u>, ATGAGTTCCTTCAGCTACGAGC, CTGGGCATCAAC GATCCAGA; <u>CAMK2A</u>, GCTCTTCGAGGAATTGGGCAA, CCTCTGAGATGCTGTCATGTAGT; <u>ALB</u>, CCTTTGGCACAATGAAGTGGGTAACC, CAGCAGTCAGCCATTTCACCATAGG; <u>CDX2</u>, CCTCTGAGATGCTGTCATGTAGT, GGTGATGTAGCGACTGTAGTGAA, <u>AFP</u>, TGTACTGCAGAGATAAGTTTAGCTGAC, CCTTGTAAGTGGCTTCTTGAACA

KD of SIX2

Gene KD was performed similar to as we previously described (Velazco-Cruz et al., 2019). pLKO.1 TRC plasmids containing shRNA sequences targeting GFP (sh-ctrl) and human SIX2 (sh-SIX2-1 and sh-SIX2-2) were received from the RNAi Core at the Washington University. sh-ctrl, GCGCGATCACATGGTCCTGCT; sh-SIX2-1, CAACGAGAACTCCAATTCTAA; sh-SIX2-2, GAGCACCTTCACAA GAATGAA. Viral particles were generated using Lenti-X 293T cells (Takara; 632180) cultured in DMEM (MilliporeSigma; D6429) with 10% heat inactivated fetal bovine serum (MilliporeSigma; F4135). Confluent Lenti-X 293T cells were transfected with 6 μg of shRNA plasmid, 4.5 μg of psPAX2 (Addgene; 12260), and 1.5 μg pMD2.G (Addgene; 12259) packaging plasmids in 600 μL of Opti-MEM (Life Technologies;31985-070) and 48 μL of Polyethylenimine 'Max' MW 40,000 Da (Polysciences; 24765-2). 16 hours post transfection media was switched. Viral containing supernatant was collected at 96 hours post transfection and concentrated using Lenti-X concentrator (Takara; 631232). Collected lentivirus was tittered using Lenti-X qRT-PCR Titration Kit (Takara; 631235). Lentiviral transduction occurred on the first day of Stage 6 by seeding 5 million dispersed single cells were into a well of a 6-well plate with lentivirus particles MOI of 5, media was switched 16 hours post transduction. psPAX2 and pMD2.G were a gift from Didier Trono.

Generation of SIX2 KO cell lines

CRISPR/Cas9 genome engineering of the HUES8 cell line was performed by the Washington University Genome Engineering & iPSC Center. The high sequence similarity with other SIX genes limited the availability of high-quality gRNA sites, making conventional frameshift introduction infeasible. Instead, a deletion strategy was employed for almost all the SIX2 coding sequence. Unique genomic regions near the start and end of the SIX2 coding sequence were identified and guide RNAs were designed; 5′ gRNA, TCGGAGCTTCGTGGGACCCGCGG and 3′gRNA, CCACGAGGTTGGCTGACATGGGG. Two homozygous SIX2 KO HUES8 cell lines were generated (KO-SIX2-1 and KO-SIX2-2). Validation of SIX2 KO was done by PCR using primers (GGGAGAACGAGTGA GAAGCG, TGCGGGTCTTTCAGTACCTG) designed to amplify a 3368 bp sequence containing the coding region, deletion of which will produce a ∼300 bp amplicon ("Deletion primers"). Validation was also done using primers (CAGTTCTGGGAGAGAAGAGAC, GGGCTGGATTCTGTTCCCATA) targeting within the SIX2 coding sequence designed to amplify 300 bp in wt and failing to amplify with successful deletion ("Inside primers"). Next generation sequencing was performed to further confirm KO.

Static glucose-stimulated insulin secretion

Measurements were performed as we previously described (Velazco-Cruz et al., 2019). The assay was performed in KRB buffer (128 mM NaCl, 5 mM KCl, 2.7 mM CaCl$_2$ 1.2 mM MgSO$_4$, 1 mM Na$_2$HPO$_4$, 1.2 mM KH$_2$PO$_4$, 5 mM NaHCO$_3$, 10 mM HEPES (GIBCO; 15630-080), and 0.1% BSA). Stage 6 clusters (∼20-30) were washed with KRB buffer and placed into transwells (Corning; 431752) with 2 mM glucose KRB. After 1 hr of equilibration, the solution was replaced with 2 mM glucose KRB for a 1 hr low glucose challenge, after which the solution was replace with 20 mM glucose alone or with

10 nM Extendin-4 (MilliporeSigma; E7144), 100 μM IBMX (MilliporeSigma; I5879), 300 μM Tolbutamide (MilliporeSigma; T0891), or 30 mM KCL (Thermo

Fisher; BP366500) KRB for a 1 hr high glucose challenge. Incubations were performed in a humidified incubator at 37°C 5% CO2. Insulin was quantified with a human insulin ELISA (ALPCO; 80-INSHU-E10.1). Cell quantification was performed by dispersing with trypLE and counting with the Vi-Cell XR.

Dynamic glucose-stimulated insulin secretion

Measurements were performed as previously described (Velazco-Cruz et al., 2019). Using an 8-channel peristaltic pump (ISMATEC; ISM931C) together with 0.015" inlet/outlet two-stop tubing (ISMATEC; 070602-04i-ND) connected to 275-μl cell chamber (BioRep; Peri-Chamber) and dispensing nozzle (BioRep; PERI-NOZZLE) using 0.04" connection tubing (BioRep; Peri-TUB-040). Solutions, tubing, and cells were maintained at 37°C using a water bath. Stage 6 clusters (∼20-30) were washed with KRB buffer and placed into perifusion cell chamber between two layers of hydrated Bio-Gel P-4 polyacrylamide beads (Bio-Rad; 150-4124). After 90 min of equilibration with 2 mM glucose KRB, cells were subjected to the following at 100 μL/min: 12 min of 2 mM glucose KRB, 24 min of 20 mM glucose KRB, and finally 12 min of 2 mM glucose KRB. Effluent was collected every 2 min. Insulin was quantified with a human insulin ELISA (ALPCO; 80-INSHU-E10.1). DNA quantification was performed by lysing the cells and measuring with the Quant-iT Picogreen dsDNA assay kit (Invitrogen; P7589). The lysis solution used consisted of 10 mM Tris (MilliporeSigma; T6066), 1 mM EDTA (Ambion; AM9261), and 0.2% Triton X-100 (Acros Organics; 327371000).

Immunostaining

Measurements were performed as we previously described (Velazco-Cruz et al., 2019). Stage 6 clusters were single-cell dispersed with trypLE, plated overnight, and fixed with 4% paraformaldehyde (Electron Microscopy Science; 15714) for 30 min at RT. Samples were treated for 30 min with blocking/permeabilizing/staining solution (5% donkey serum (Jackson Immunoresearch; 017-000-121) and 0.1% Triton X-100 (Acros Organics; 327371000) in PBS). Samples were then incubated overnight at 4°C with primary antibody diluted in staining solution, incubated 2 hr at 4°C with secondary antibodies diluted in staining solution, and stained with DAPI for 5 min. Nikon A1Rsi confocal microscope or Leica DMI4000 fluorescence microscope were used to take images. The antibodies used are listed in Table S4.

Flow cytometry

Measurements were performed as we previously described (Velazco-Cruz et al., 2019). Clusters were single-cell dispersed with TrypLE, fixed with 4% paraformaldehyde for 30 min at 4°C, incubated 30 min at 4°C in blocking/permeabilizing/staining solution, incubated with primary antibodies in staining buffer overnight at 4°C, incubated with secondary antibodies in staining buffer for 2 hr at 4°C, resuspended in staining buffer, and analyzed on an LSRII (BD Biosciences) or X-20 (BD Biosciences). Dot plots and percentages were generated using FlowJo. The antibodies used are listed in Table S4.

RNA sequencing

RNA from sh-ctrl and sh-SIX2-1 transduced cells (n = 6 per condition) was extracted on Stage 6 Day 12 using RNeasy Mini Kit with DNase treatment. Washington University Genome Technology Access Center performed library preparation, sequencing, and determination of differential expression. Libraries were indexed, pooled, and single-end 50 base pair reads were sequenced on one lane of an Illumina HiSeq 3000 generating 25-30 million reads per sample. Reads were then aligned to the Ensembl release 76 top-level assembly with STAR. Gene counts were derived from the number of uniquely aligned unambiguous reads by Subread:featureCount. All gene counts were imported into EdgeR5 and TMM normalization size factors were calculated. Ribosomal genes and genes not expressed in the smallest group size minus one, samples greater than one count-per-million were excluded from further analysis. The TMM size factors and the matrix of counts were imported into Limma6. Weighted likelihoods based on the observed mean-variance relationship of every gene and sample were calculated for all samples with the voomWithQualityWeights7. Differential expression analysis was performed with a Benjamini-Hochberg false-discovery rate adjusted p values cut-off of less than or equal to 0.05. Hierarchical clustering and heatmaps were generated using Morpheus (https://software.broadinstitute.org/morpheus). To perform gene set enrichment analyses normalized all gene counts were imported into GSEA software and the Molecular Signature Database (MSigDB) Hallmark, KEGG, and Gene Ontology gene libraries were used to identify enriched gene sets (Subramanian et al., 2005). *In Vitro* Beta Cell Maturation gene set was generated by combining Veres et al. (Veres et al., 2019) Stage 6 enriched genes logbase2 fold or greater (76 genes), and Nair et al. (Nair et al., 2019) β-clusters enriched genes (424 genes) with SIX2 removed.

Hormone content measurements

Measurements were performed as we previously described (Velazco-Cruz et al., 2019). Stage 6 cell clusters were collected, washed with PBS, placed in acid-ethanol solution (1.5% HCl and 70% ethanol), stored at −20°C for 24 hours, vortexed, returned to −20°C for 24 additional hours, vortexed, and centrifuged at 2100 G for 15 min. The supernatant was collected and neutralized with an equal volume of 1 M TRIS (pH 7.5). Human insulin and pro-insulin content were quantified using Human Insulin ELISA and Proinsulin ELISA (Mercodia; 10-1118-01) respectively. Samples were normalized to cell counts made using the Vi-Cell XR.

OCR and ECAR measurements

Measurements were performed similar to as we previously reported (Millman et al., 2019). Stage 6 cell clusters were dispersed into a single-cell suspension and plated 200,000 per well. After overnight incubation in S6 media, the media was replaced with RPMI-1640 (Sigma; R6504) with 7.4 pH and 20 mM glucose. The Seahorse XFe24 flux analyzer (Agilent) was used to measure OCR and ECAR. After basal measurements, 3 μM oligomycin (Calbiochem; 1404-19-9), 0.25 μM carbonyl cyande-4-(trifluoromethoxy) phenylhydrazone (FCCP) (Sigma; 270-86-5), and 1 μM rotenone (Calbiochem; 83-79-4) and 2 μM antimycin A (Sigma; 1397-94-0) where injected sequentially and replicate measurements performed.

Cytoplasmic calcium measurements

Calcium measurements were done similar as previously reported (Kenty and Melton, 2015; Pagliuca et al., 2014). Stage 6 day 12 clusters were single cell dispersed by incubation in TrypLE for 10 minutes and plated down onto a Matrigel coated #1.5 glass bottom 96 well plate (Cellvis; 963-1.5H-N) and allowed to attach overnight. Following overnight attachment clusters were washed twice with 2 mM glucose KRB and incubated in 2 mM glucose KRB with 20 μM Fluo-4 AM (Invitrogen; F14201) for 45 min at 37°C. Cells were washed twice with 2 mM glucose KRB, placed in 2 mM glucose KRB and incubated for 10 min at 37°C, then placed in a 37°C 5% CO_2 humidified Tokai-hit stage-top on a Nikon Eclipse Ti inverted spinning disk confocal equipped with a Yokagawa CSU-X1 variable speed Nipkow spinning disk scan head equipped with a motorized xy stage including nano-positioning piezo z-insert. Images were acquired with the cells at 2 mM glucose KRB, 20 mM glucose KRB, and 20 mM glucose 30 mM KCl KRB. Analysis of calcium flux image stack was performed using ImageJ with the StackReg package for correction.

QUANTIFICATION AND STATISTICAL ANALYSIS

GraphPad Prism was used to calculate statistical significance for all non-RNA sequencing data. One- or two-sided paired or unpaired t tests were used.

Differential expression analysis of RNA sequencing data was performed with a Benjamini-Hochberg false-discovery rate adjusted p values cut-off of less than or equal to 0.05.

Error bars represent s.e.m. unless otherwise noted. Sample size (n) is specified in each figure caption and indicates biological replicates unless otherwise noted. Statistical parameters are stated in figure captions.

Supplemental Information

SIX2 Regulates Human β Cell Differentiation from

Stem Cells and Functional Maturation _In Vitro_

Leonardo Velazco-Cruz, Madeleine M. Goedegebuure, Kristina G. Maxwell, Punn Augsornworawat, Nathaniel J. Hogrebe, and Jeffrey R. Millman

Supplementary Figures

A
HUES8 hESC

Relative SIX2 Expression vs sh-ctrl, sh-SIX2-1, sh-SIX2-2

1013-4FA hiPSC

SIX2 Relative Expression vs sh-ctrl, sh-SIX2-1

B
CP SIX2 DAPI

sh-ctrl   sh-SIX2-1

20 μm

C
20mM Glucose

Insulin Secretion (μIU / μg DNA) vs Time (Minutes)

sh-ctrl
sh-SIX2-2

D
Glucose
2mM
20mM

Insulin Secretion (μIU/ 10^6 Cells) vs sh-ctrl, sh-SIX2-2

E
1013-4FA

20mM Glucose

Insulin Secretion (μIU/μg DNA) vs Time (Minutes)

sh-ctrl
sh-SIX2-1

F
1013-4FA

2mM
20mM

Insulin Secretion (μIU/10^6 cells) vs sh-ctrl, sh-SIX2-1

G

Deletion.Primer.F   5' gRNA

SIX2 Coding Sequence

4,000

Deletion.Primer.R

Inside.Primer.F   Inside.Primer.R

3' gRNA

H
Deletion Primers   Inside Primers

100bp wt   KO1 KO2   wt   KO1 KO2

I
gggggttcggagcttcgtgggacctgtcagccaacctcgtggacctgggctcctagaacccatt
cccccaagcctcgaagcaccctggacagtcggttggagcacctggacccgaggatcttgggtaa

5' gRNA

285   290
S A N L V D L G S *
SIX2

285   290
S A N L V D L G S *
SIX2

3' gRNA

gggggttcggagcttcgtgggacctgtcagccaacctcgtggacctgggctcctagaacccatt

GGGGTTCGGAGCTTCGTGG----------ACCTGGGCTCCTAGAACCCATT   KO-SIX2-1 allele #1
GGGGTTCGGAGCTTCGTGGGACCTG--------------------GGCTCCTAGAACCCATT   KO-SIX2-1 allele #2
GGGGTTCGGAGCTTCGTGGGACC--AGCCAACCTCGTGGACCTGGGCTCCTAGAACCCATT   KO-SIX2-2 allele #1
GGGGTTCGGAGCTTCGTGGGACC--GTCAGCCAACCTCGTGGACCTGGGCTCCTAGAACCCATT   KO-SIX2-2 allele #2

Indels

J
SIX2 Relative Expression vs SIX2 WT, SIX2 KO

K
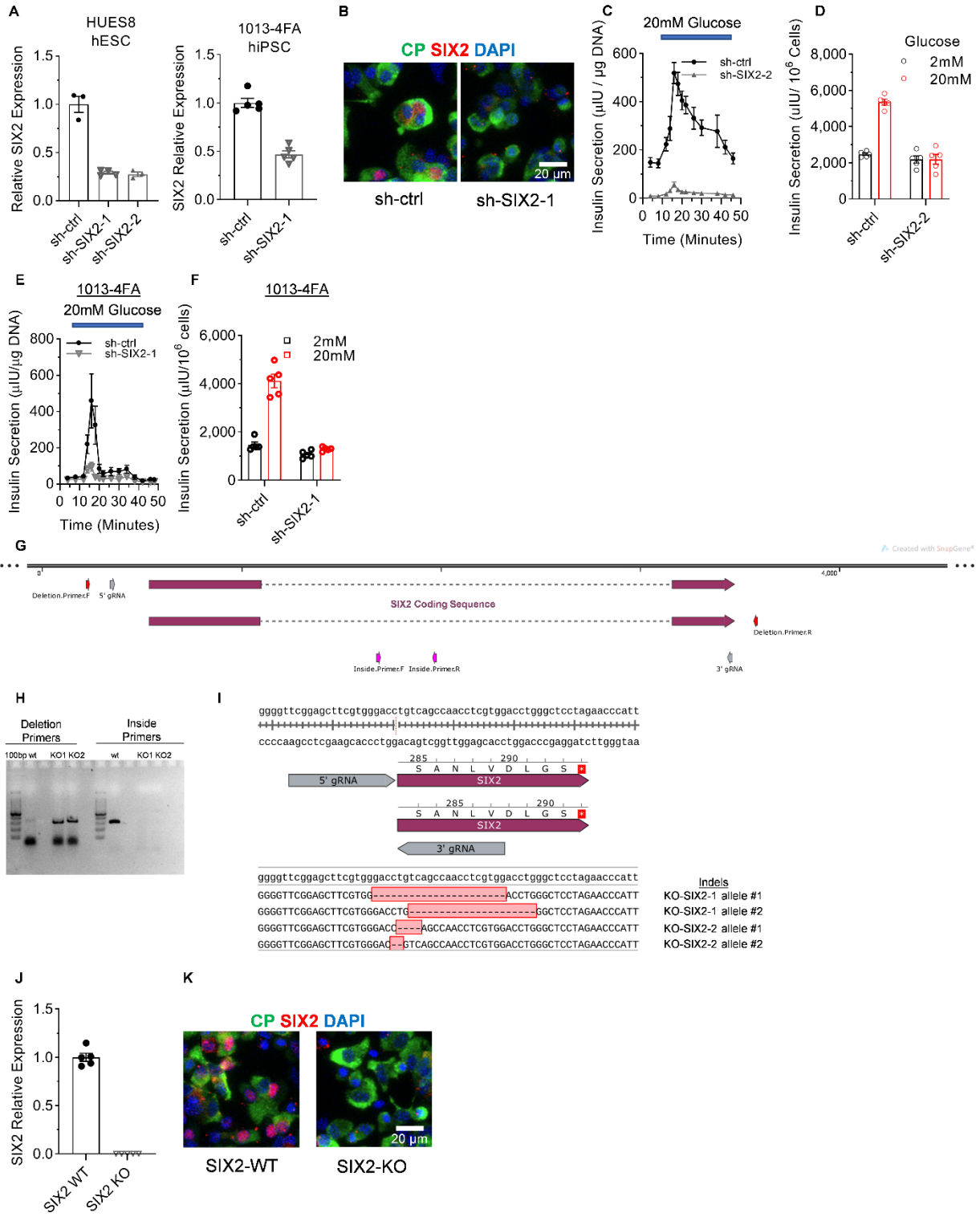CP SIX2 DAPI

SIX2-WT   SIX2-KO

20 μm

Figure S1. Validation of SIX2 KD and KO assessments. Related to Figure 1. (**A**) Real-time PCR measurements of SIX2 gene expression for Stage 6 cells transduced with sh-ctrl, sh-SIX2-1, or sh-SIX2-2 for differentiated HUES8 (left) or 1013-4FA, made with protocol 2, (right) cells. n=3. (**B**) C-peptide and SIX2 immunostaining of stage 6 cells made with protocol 2 transduced with sh-ctrl or sh-SIX2-1 in the 1013-4FA background. (**C**) Dynamic glucose-stimulated insulin secretion of Stage 6 HUES8 cells transfected with control shRNA (sh-ctrl; n=4) or shRNA targeting SIX2 (sh-SIX2-2; n=4). Cells are perfused with 2 mM glucose except when indicated in a perifusion chamber. (**D**) Static glucose-stimulated insulin secretion of sh-ctrl or sh-SIX2-2 transduced Stage 6 HUES8 cells. n=5. (**E**) Dynamic glucose-stimulated insulin secretion of Stage 6 1013-4FA cells made with protocol 2 transfected with control shRNA (sh-ctrl; n=4) or shRNA targeting SIX2 (sh-SIX2-1; n=4). Cells are perfused with 2 mM glucose except when indicated in a perifusion chamber. (**F**) Static glucose-stimulated insulin secretion of sh-ctrl or sh-SIX2-1 transduced Stage 6 1013-4FA cells made with protocol 2. n=5. (**G**) CRISPR knock out strategy for the generation of the SIX2 KO HUES8 cell lines KO-SIX2-1 and KO-SIX2-2. HUES8 homozygous SIX2 KO clones were generated by deleting the SIX2 coding sequence using two gRNAs target flanking regions of the SIX2 coding sequence. Also shown are the primers used to validate deletion, "deletion primers" and "inside primers". (**H**) PCR of SIX2 KO clones confirming SIX2 coding sequence deletion. "Deletion primers" will produce 3368 bp amplicon for wt but only ~300 bp amplicon with successful deletion. "Inside primers" will produce ~300 bp amplicon for wt but fail to amplify with successful deletion. (**I**) Next generation sequencing confirming deletion of SIX2 coding sequence in KO cell lines. The entire sequence between the 5' and 3' gRNA was absent (marked with red dash in reference). 1,085 total reads for KO-SIX2-1 clone and 840 total reads for KO-SIX2-2 clone were sequenced and 0% wt gRNA target sequence were detected and frame shifting indels totaled 100% for both clones. A few bp of SIX2 coding are leftover. (**J**) Real-time PCR measurements of SIX2 gene expression for Stage 6 cells made with protocol 2 from wt or KO SIX2 HUES8 backgrounds. n=5. (**K**) C-peptide and SIX2 immunostaining of Stage 6 cells made with protocol 2 from wt or KO SIX2 HUES8 backgrounds. Error bars represent s.e.m.
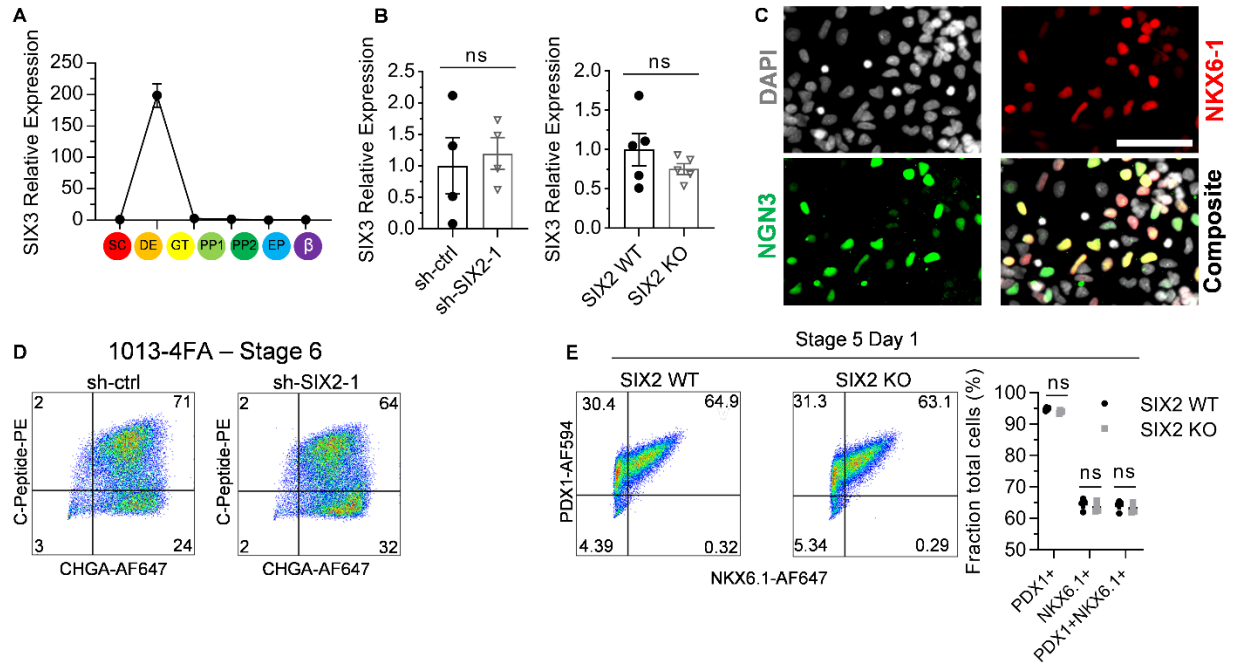
Figure S2. Additional evaluation of SIX3 and SIX2. Related to Figure 2. (**A**) Real-time PCR measurements of SIX3 in undifferentiated hESCs and at the end of each stage of the differentiation. Data is presented as the fold change relative to Stage 6 cells. All n=6, except PP2 n=3. (**B**) Real-time PCR measurements of SIX3 gene expression for Stage 6 cells transduced with sh-ctrl or sh-SIX2-1 (n=4; left) or SIX2 wt and KO cells (n=5; right). ns=p>0.05. (**C**) Immunostaining of NGN3 and NKX6-1 3 days into Stage 5. Scale bar=25 μm. (**D**) Flow cytometry plots of Stage 6 cells made with protocol 2 from the 1013-4FA background transduced with shRNA against GFP (control) and SIX2. (**E**) Flow cytometry plots of Stage 5 day 1 cells made with protocol 2 from the HUES8 background wt or KO for SIX2. n=4. ns by unpaired two-way t test. Error bars represent s.e.m.

A

■ sh-ctrl enriched

KEGG

- TYPE_I_DIABETES_MELLITUS
- MATURITY_ONSET_DIABETES_OF_THE_YOUNG
- SNARE_INTERACTIONS_IN_VESICULAR_TRANSPORT
- PROTEIN_EXPORT
- MAPK_SIGNALING_PATHWAY
- CALCIUM_SIGNALING_PATHWAY

NES (0.0, 0.5, 1.0, 1.5)

Hallmark

- PANCREAS_BETA_CELLS
- OXIDATIVE_PHOSPHORYLATION
- IL6_JAK_STAT3_SIGNALING
- UNFOLDED_PROTEIN_RESPONSE
- HEDGEHOG_SIGNALING

NES (0.0, 0.5, 1.0, 1.5, 2.0)

Gene Ontology

- ENDOPLASMIC_RETICULUM_UNFOLDED_PROTEIN_RESPONSE
- CALMODULIN_DEPENDENT_PROTEIN_KINASE_ACTIVITY
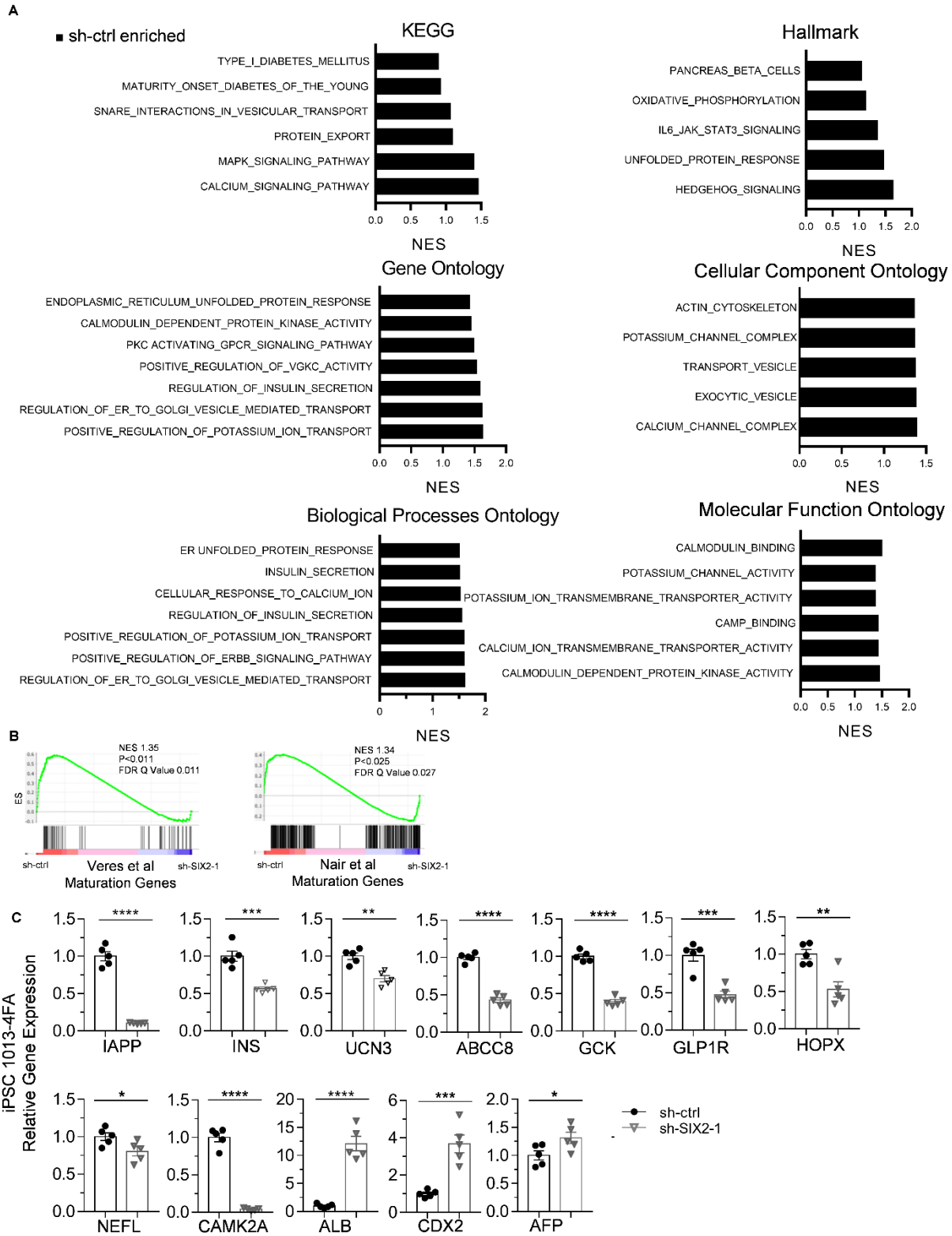- PKC ACTIVATING_GPCR_SIGNALING_PATHWAY
- POSITIVE_REGULATION_OF_VGKC_ACTIVITY
- REGULATION_OF_INSULIN_SECRETION
- REGULATION_OF_ER_TO_GOLGI_VESICLE_MEDIATED_TRANSPORT
- POSITIVE_REGULATION_OF_POTASSIUM_ION_TRANSPORT

NES (0.0, 0.5, 1.0, 1.5, 2.0)

Cellular Component Ontology

- ACTIN_CYTOSKELETON
- POTASSIUM_CHANNEL_COMPLEX
- TRANSPORT_VESICLE
- EXOCYTIC_VESICLE
- CALCIUM_CHANNEL_COMPLEX

NES (0.0, 0.5, 1.0, 1.5)

Biological Processes Ontology

- ER UNFOLDED_PROTEIN_RESPONSE
- INSULIN_SECRETION
- CELLULAR_RESPONSE_TO_CALCIUM_ION
- REGULATION_OF_INSULIN_SECRETION
- POSITIVE_REGULATION_OF_POTASSIUM_ION_TRANSPORT
- POSITIVE_REGULATION_OF_ERBB_SIGNALING_PATHWAY
- REGULATION_OF_ER_TO_GOLGI_VESICLE_MEDIATED_TRANSPORT

NES (0, 1, 2)

Molecular Function Ontology

- CALMODULIN_BINDING
- POTASSIUM_CHANNEL_ACTIVITY
- POTASSIUM_ION_TRANSMEMBRANE_TRANSPORTER_ACTIVITY
- CAMP_BINDING
- CALCIUM_ION_TRANSMEMBRANE_TRANSPORTER_ACTIVITY
- CALMODULIN_DEPENDENT_PROTEIN_KINASE_ACTIVITY

NES (0.0, 0.5, 1.0, 1.5, 2.0)

B

NES 1.35
P<0.011
FDR Q Value 0.011

sh-ctrl — Veres et al Maturation Genes — sh-SIX2-1

NES 1.34
P<0.025
FDR Q Value 0.027

sh-ctrl — Nair et al Maturation Genes — sh-SIX2-1

C

iPSC 1013-4FA Relative Gene Expression

IAPP (****), INS (***), UCN3 (**), ABCC8 (****), GCK (****), GLP1R (***), HOPX (**)

NEFL (*), CAMK2A (****), ALB (****), CDX2 (***), AFP (*)

● sh-ctrl
▽ sh-SIX2-1

Figure S3. Additional RNA sequencing analysis. **Related to Figure 3.** (**A**) Enriched gene sets for important β cell processes from the Molecular Signatures Database. (**B**) Additional enrichment plots. These are made with genes from

the individual custom gene sets comprising 76 genes identified in Veres et al (Veres et al., 2019) and the top 424 genes identified in Nair et al (Nair et al., 2019) positively correlating with time and maturation in vitro (Tables S2-S3). (**C**) Real-time PCR measurements of Stage 6 cells made with protocol 2 transduced with sh-ctrl or sh-SIX2-1 in the 1013-4FA background. $*p<0.05$, $**p<0.01$, $***p<0.001$, $****p<0.0001$ by two-way unpaired t test. Error bars represent s.e.m.
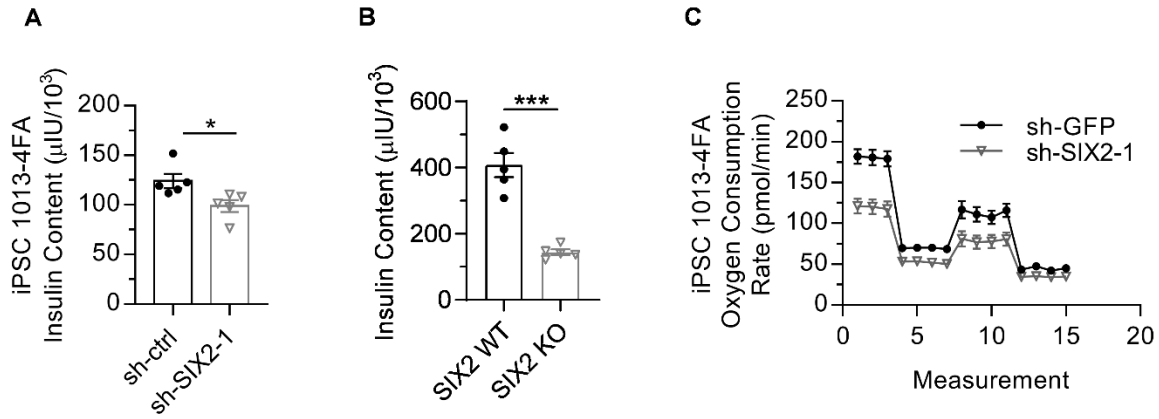
Figure S4. Additional data on SIX2 KD and KO effects on SC-β cells. Related to Figure 4. (**A**) Insulin content for Stage 6 cells transduced with sh-ctrl or sh-SIX2-1 in the 1013-4FA background. n=5. (**B**) Insulin content for Stage 6 cells wt or KO for SIX2. n=5. (**C**) OCR measurements for Stage 6 cells transduced with sh-ctrl or sh-SIX2-1 in the 1013-4FA background under basal conditions and after sequential injections of Oligomycin (OM), Carbonyl cyanide-*4*-(trifluoromethoxy)phenylhydrazone (FCCP), and Antimycin A with rotenone (AA/R). n=9 for sh-ctrl and n=10 for sh-SIX2-1. *p<0.05,***p<0.001 by two-way unpaired t test. Error bars represent s.e.m.